Effect of low-temperature annealing on void-related microstructure in amorphous silicon: A computational study

View the article online for updates and enhancements.

IOP ebooks™

Bringing you innovative digital publishing with leading voices to create your essential collection of books in STEM research.

Start exploring the collection - download the first chapter of every title for free.

Effect of low-temperature annealing on void-related microstructure in amorphous silicon: A computational study

Durga Paudel[†]**, Raymond Atta-Fynn**[∗]**, D. A. Drabold**[‡] **and Parthapratim Biswas**[†]

[†] Department of Physics and Astronomy, The University of Southern Mississippi, Hattiesburg, MS 39406, USA
[∗] Department of Physics, University of Texas, Arlington, TX 76019, USA
[‡] Department of Physics and Astronomy, Ohio University, Athens, Ohio 45701, USA

E-mail: `partha.biswas@usm.edu`

Abstract.   We present a computational study of void-induced microstructure in amorphous silicon (a-Si) by generating ultra-large models of a-Si with a void-volume fraction of 0.3%, as observed in small-angle X-ray scattering (SAXS) experiments. The relationship between the morphology of voids and the intensity of scattering in SAXS has been studied by computing the latter from the Fourier transform of the reduced pair-correlation function and the atomic-form factor of amorphous silicon. The effect of low-temperature annealing on scattering intensities and the microstructure of voids has been addressed, with particular emphasis on the shape and size of voids, by studying atomic rearrangements on void surfaces and computing the average radius of gyration of the voids from the spatial distribution of surface atoms and the intensity plots in the Guinier approximation. The study suggests that low-temperature annealing can lead to considerable restructuring of void surfaces, which is clearly visible from the three-dimensional shape of the voids but it may not necessarily reflect in one-dimensional scattering-intensity plots.

1. Introduction

The microstructure of small- and large-scale inhomogeneities, such as multi-vacancies and voids, plays an important role in the determination of structural and optoelectronic properties of pure and hydrogenated amorphous silicon. The presence of voids in amorphous silicon (a-Si) and germanium (a-Ge) was postulated in the late 1960s by Brodsky and Title [1] and Moss and Graczyk [2], with the aid of electron spin resonance (ESR) and small-angle electron diffraction measurements, respectively, to explain the low mass density of amorphous Si/Ge (by about 10–15%) from their crystalline counterpart. In the intervening decades, a number of experimental techniques, ranging from small-angle X-ray scattering (SAXS) [3], spectroscopic ellipsometry (SE) and Fourier transform infrared spectroscopy (FTIR) [4] and effusion of hydrogen and implanted-helium measurements [5] in a-Si:H to nuclear magnetic resonance (NMR) [6], provided an impressive database of experimental information on structural properties of a-Si and its hydrogenated counterpart. By contrast, theoretical efforts [7–10] to address structural and electronic properties of a-Si so far have been mostly limited to results obtained from small atomistic models, consisting of a few to several hundreds of atoms, depending upon the quantum-mechanical or classical nature of atomic interactions employed in building those models. Computational modeling of large-scale inhomogeneities in amorphous networks, such as voids in a-Si and a-Ge, were particularly hindered in the past due to the absence of large realistic models that were

needed to take into account the size and number density of voids, as observed in SAXS, NMR and FTIR studies. Since voids are nanoscale inhomogeneities, with a diameter ranging from 10–40 Å and a void-volume fraction of 0.1–0.4%, it is necessary to produce ultra-large models, consisting of 10^5 atoms or more, so that the models are not only experimentally compliant but also statistically reliable and capable of producing configurational-averaged values of physical properties. In this communication, we address the structure of void-induced microstructure in a-Si by carrying out realistic simulations of voids, using classical molecular-dynamics simulations.

Of particular interest is the evolution of the microstructure of voids in a-Si/a-Si:H, induced by thermal annealing. While it is known that low-temperature annealing increases structural ordering in a-Si, as observed in Raman spectroscopy [11], the effect of annealing on the shape and size of voids is still largely unknown. Since the restructuring of atoms in the vicinity of void surfaces, especially in a-Si:H, is intrinsically connected with the photovoltaic behavior of a-Si:H-based solar devices, computational studies of the relaxation behavior of atoms on and near void surfaces are of paramount importance. Here, we present a quantitative study of characterization of void shapes and sizes upon low-temperature annealing by examining spatial distributions of void-surface atoms and computing the scattering intensity in SAXS, produced by the voids of evolving shape present in the models. Below, we briefly present the computational method, followed by results and conclusions of our work.

2. Computational Method

Since scattering contributions in SAXS chiefly originate from the small wave-vector region ($k \leq 1$ Å^{-1}), it is essential to extract information on the extended-scale inhomogeneities by generating large models of a-Si for realistic simulation of scattering intensity in the small-angle region. Toward that end, we generated two independent a-Si models (M1 and M2), consisting of 262,400 atoms in a cubic box of length 176.123 Å, using the modified Stillinger-Weber potential [12] via molecular-dynamics (MD) simulations in canonical ensembles. The MD simulations comprised the following steps: a) equilibration of an initial random configuration at 1800 K for 40 ps; b) gradual cooling of the equilibrated system from 1800 K to 300 K in steps of 100 K per 25 ps so that the total simulation time is 415 ps per cooling cycle; c) repetition of step (b) for up to 40 cycles until a high-quality amorphous network could form which was characterized by a narrow bond-angle distribution and a small percentage of coordination defects; d) total-energy relaxations of the system at 300 K, using the limited-memory BFGS method [13] to obtain the nearest local minimum-energy configuration.

In order to study the temperature dependence of SAXS intensity and void shape, we generated four additional models from M1 and M2 by introducing ellipsoidal voids such that the total void-volume fraction, f_v, corresponds to 0.3%, as observed in experiments [14]. The ellipsoidal voids were generated randomly so that they were sparsely distributed within amorphous networks with a minimum surface-to-surface distance of 6 Å between any two neighboring voids. An axial ratio of $a : b : c = 0.5 : 1 : 2$, with a length scale of $b = 6$ Å, was employed to generate ellipsoidal voids and silicon atoms in the region between x and $x + d$, where $x = (a, b, c)$ and $d = 2.8$ Å, were marked as surface atoms in order to monitor the evolution of void shape upon annealing and relaxation. Two independent sets of models were studied to examine the effect of annealing on void shape and the intensity of scattering at 400 K and 600 K. The corresponding relaxed models were also examined in our work.

The computation of scattering intensity in SAXS follows directly from the static structure factor, $S(k)$, and the atomic-form factor, $f(k)$, of a-Si. By invoking the homogeneous approximation, the structure factor can be written as,

$$S(k) = 1 + \frac{1}{k} \int_0^{R_c} G(r) \sin kr \, dr. \tag{1}$$

Here, $G(r)$ is the reduced pair-correlation function (PCF) and k is the magnitude of wave-vector transfer, $k = 4\pi \sin(\theta)/\lambda$, where 2θ is the scattering angle and λ is the wavelength of X-ray. The upper limit of the integral in Eq. (1) is chosen so that $G(r)$ can be neglected for $r > R_c = 30$ Å. Denoting $f(k)$ as the

Table 1. Structural properties of simulated a-Si models. L, N, ρ, C_4, C_3, r_{avg}, θ_{avg} and $\Delta\theta$ are the size of the simulation cell, total number of atoms, mass density, four-fold coordination, three-fold coordination, average bond length, average bond angle and the RMS fluctuation of the bond angles, respectively.

Models	N	L (Å)	ρ (g.cm^{-3})	C_4 (%)	C_3 (%)	r_{avg} (Å)	θ_{avg} (deg.)	$\Delta\theta$ (deg.)
M1	262,400	176.12	2.24	97.65	1.27	2.39	109.24	9.10
M2	262,400	176.12	2.24	97.71	1.27	2.39	109.25	9.08

atomic-form factor, the scattering intensity, $I(k)$, can be written as, $I(k) = \frac{1}{N}|f(k)|^2 S(k)$, where N is the total number of atoms.
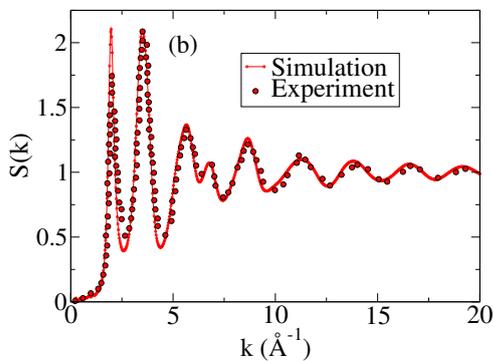
3. Results and Discussions

Figure 1. The static structure factor of a-Si from simulations (M1+M2) and experiments. Experimental data are from in Ref. [15].

Table 1 lists the characteristic structural properties of M1 and M2 models, obtained from molecular-dynamics (MD) simulations. Given the ultra-large size of the models, it is remarkable that the concentration of coordination defects and the root-mean-square (RMS) deviation of bond angles are less than 2.4% and 10°, respectively. Figure 1 shows the structure factor of the simulated models, averaged over M1 and M2 models, along with the experimental structure-factor data from wide-angle X-ray diffraction measurements [15]. The simulated values of the structure factor match closely with the experimental data, indicating that the models are not only fully consistent with two- and three-body correlation functions but also have a very low concentration of coordination defects. To our knowledge, these ultra-large classical MD models are among the very best models of a-Si, with 10^5 or more atoms, so far reported in the literature.

The effect of low-temperature annealing on the shape and size of voids was studied by analyzing results from real and reciprocal spaces. Figure 2(a) depicts the evolution of an ellipsoidal void at 400 K and 600 K, along with the original shape, all superimposed on each other. The distorted ellipsoidal surfaces observed at 400 K and 600 K are shown in green and red colors, respectively, whereas the original void surface is shown in blue color. The striking color patches, which originate from the superposition of three ellipsoidal surfaces, are reflective of the degree of reconstruction of the surface at 400 K and 600 K. These surfaces were generated from the position coordinates of the respective void-surface atoms, using an identical set of iso-surface parameters in VMD software. To obtain a quantitative estimate of surface reconstruction, the distributions of atomic displacements (u) of the surface atoms of the ellipsoidal void at 600 K and 400 K are plotted in Fig. 2(b). While it is evident from Fig. 2(b) that majority of the surface atoms have displaced from their original position by a distance of 0–0.75 Å, a small number of atoms have moved more than 1.0 Å, causing considerable restructuring of the void surface. This observation has been found to be true for other ellipsoidal voids as well.

While an analysis of three-dimensional distribution of atoms clearly reveals atomic rearrangements on void surfaces, a question of considerable importance, from the point of view of SAXS, is to what extent these temperature-induced structural changes can be reflected in $I(k)$-vs-k plots. Since SAXS essentially provides scalar information or *one-dimensional* physical quantities, such as scattering intensities and the average radius of gyration of the voids in the Guinier approximation [16], it is pertinent to examine whether these scalar quantities are sensitive to structural changes observed on void surfaces. Figure 2(c) shows the scattering intensities obtained from the original model with voids (blue) and the
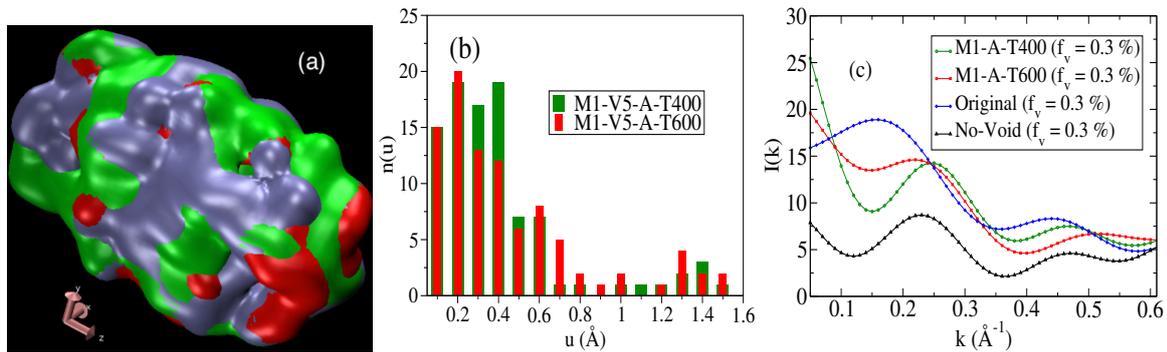
Figure 2. (a) The changing shape of an ellipsoidal void (M1-V5) in M1 model at two different annealing temperatures. Red and green colors correspond to the shape at temperature 600 K and 400 K, respectively, along with the original ellipsoid in blue color. The color patches are indicative of surface reconstruction, showing the evolving shape of the void with temperature. (b) The distribution of atomic displacements (u) of the surface atoms on the ellipsoidal void, as shown in Fig. 2(a), annealed at 400 K (green) and 600 K (red). (c) The simulated values of the scattering intensity at 400 K and 600 K with and without voids, as indicated in the plot.

corresponding annealed models at 600 K (red) and 400 K (green). For comparison, we have also included the intensity values obtained from the original model with no voids (black). A few observations immediately follow from Fig. 2(c). First, an excess of small-angle scattering is apparent in the computed values of the scattering intensity from the models with voids (red/green/blue), compared with the one with no voids (black). Second, the variation of the scattering intensity in the presence of voids is only pronounced in the small-k region below 0.25 Å^{-1}. Since the wave-vector region below 0.1 Å^{-1} is not very reliable, due to the presence of numerical noise at large distances in $G(r)$ (see Eq. 1), it would not be inappropriate to conclude that the changes are somewhat weakly reflected in the intensity plots as far as our simulations are concerned. Third, this conclusion is consistent with the values of the radius of gyration, obtained from *real-space* distribution of surface atoms. Table 2 lists R_g values obtained from the spatial distribution of void-surface atoms at 400 K and 600 K, which are quite close to each other. On the other hand, the radius of gyration, r_g, obtained from the intensity plots in the Guinier approximation [16], shows a noticeable variation with temperature. Since the Guinier approximation entails expressing $I(k) \approx \exp(-k^2 r_g^2/3)$ in the limit $k \to 0$ and fitting the intensity values on a semi-log plot, $\ln I(k)$-vs-k^2, r_g values obtained from this approach is quite sensitive to the computed values of the intensity and the small-k region employed in the calculations. Here, we have employed intensity values in the region, $0.015 \le k^2 \le 0.16$ Å^{-1}, to obtain the r_g values presented in Table 2. In Fig. 3, we have presented the corresponding shape, atomic displacements and the values of the scattering intensities obtained by relaxing the annealed models at temperature 400 K and 600 K. Although considerable changes in the shape of the relaxed ellipsoidal void can be seen in Fig. 3(a), the scattering intensities in Fig. 3(c) appear to be not very susceptible to these changes on void surfaces.

4. Conclusions

In this paper, we have studied the microstructure of nanometer-size voids, by simulating ultra-large models of a-Si, using classical molecular-dynamics simulations. The intensity of small-angle X-ray scattering, produced by ellipsoidal voids present in the models, is computed from the Fourier transform of the reduced pair-correlation function and the atomic-form factor of silicon in an effort to study the effect of low-temperature annealing of up to 600 K on the morphology, especially the shape and size, of the voids. Our study shows that thermalization of the models at 600 K produces considerable restructuring of void surfaces with atomic displacements of the surface atoms as high as 1.6 Å. The reconstruction of void surfaces has been found to be somewhat weakly reflected in one-dimensional scattering plots, obtained from the simulated values of the scattering intensity produced by the models. It has been observed that,
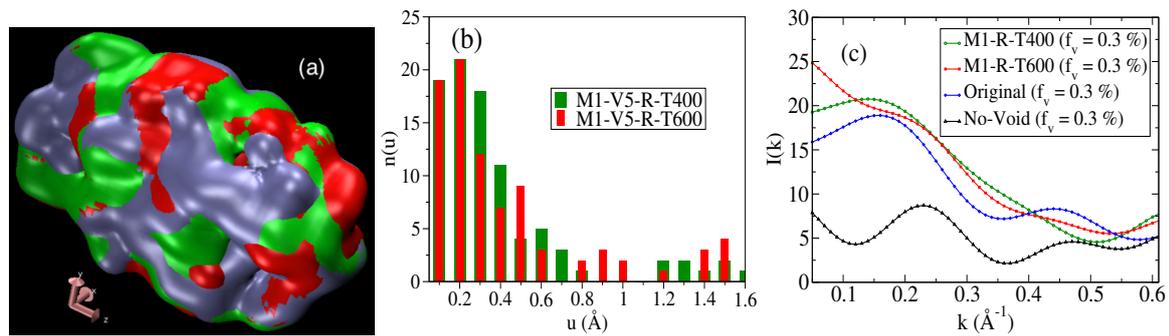
Figure 3. (a) The shape of the same ellipsoidal void obtained after relaxation of the annealed model (in Fig. 2a) at 400 K (green) and 600 K (red). (b) The distributions of atomic displacements (u) of the atoms on the ellipsoidal void surface with the same color code as in (a). (c) The scattering intensities from the relaxed models at 400 K and 600 K.

Table 2. Characteristic properties of void distributions in annealed models of a-Si. R_g, σ and r_g indicate the average gyrational radius, the root-mean-square fluctuation of R_g and the Guinier radius from the scattering intensity plots in Fig. 2(c), respectively. A/R-T400 corresponds to the annealed/relaxed model at 400 K.

Models	$R_g \pm \sigma$ (Å)	r_g (Å)	Models	$R_g \pm \sigma$ (Å)	r_g (Å)
M1-A-T400	5.87±0.12	3.64	M1-R-T400	5.88±0.11	4.42
M1-A-T600	5.84±0.12	5.19	M1-R-T600	5.86±0.12	4.85
M2-A-T400	5.94±0.07	4.66	M2-R-T400	5.96±0.08	4.53
M2-A-T600	5.92±0.1	5.87	M2-R-T600	5.94±0.1	5.33

despite considerable changes of void shape, one-dimensional measures of size, such as gyrational and Guinier radii – obtained from the spatial distribution of atoms and the intensity plots, respectively – are not particularly affected by low-temperature annealing.

References
[1] Brodsky M H and Title R S 1969 *Phys. Rev. Lett.* **23**(11) 581–585
[2] Moss S C and Graczyk J F 1969 *Phys. Rev. Lett.* **23**(20) 1167–1171
[3] Mahan A H, Williamson D L, Nelson B P and Crandall R S 1989 *Phys. Rev. B* **40**(17) 12024–12027
[4] Liu W, Zhang L, Meng F, Guo W, Bao J, Liu J, Wang D and Liu Z 2015 *Scripta Materialia* **107** 50 – 53
[5] Beyer W 2004 *Physica Status Solidi (c)* **1** 1144–1153
[6] Boyce J B and Stutzmann M 1985 *Phys. Rev. Lett.* **54**(6) 562–565
[7] Biswas P, Paudel D, Atta-Fynn R, Drabold D A and Elliott S R 2017 *Phys. Rev. Applied* **7**(2) 024013
[8] Biswas P and Elliott S R 2015 *Journal of Physics: Condensed Matter* **27** 435201
[9] Biswas P, Drabold D A and Atta-Fynn R 2014 *Journal of Applied Physics* **116** 244305
[10] Brahim R B and Chehaidar A 2011 *Journal of Non-Crystalline Solids* **357** 2620 – 2625
[11] Hishikawa Y 1987 *Journal of Applied Physics* **62** 3150–3155
[12] Vink R, Barkema G, van der Weg W and Mousseau N 2001 *Journal of Non-Crystalline Solids* **282** 248 – 255
[13] Nocedal J 1980 *Mathematics of Computation* **35** 773–782
[14] Williamson D, Mahan A, Nelson B and Crandall R 1989 *Journal of Non-Crystalline Solids* **114** 226 – 228
[15] Laaziri K, Kycia S, Roorda S, Chicoine M, Robertson J L, Wang J and Moss S C 1999 *Phys. Rev. Lett.* **82**(17) 3460–3463
[16] Guinier A 1994 *X-Ray Diffraction In Crystals, Imperfect Crystals, and Amorphous Bodies* (Dover Publications, Inc., New York) ISBN 13:978-0-486-68011-8